RSC Advances

ROYAL SOCIETY OF CHEMISTRY

www.rsc.org/advances

Cite this: DOI: 10.1039/c0xx00000x

www.rsc.org/xxxxxx

ARTICLE TYPE

All carbon nanotube based flexible field emission devices prepared through a film transfer method

Jinzhuo Xu[a], Peng Xu[c], Pingsheng Guo[a,*], Wei Ou-Yang[a,*], Yiwei Chen[a], Tao Feng[a,b], Xianqing Piao[a], Miao Wang[c] and Zhuo Sun[a]

Received (in XXX, XXX) Xth XXXXXXXXX 20XX, Accepted Xth XXXXXXXXX 20XX

DOI: 10.1039/c0xx00000x

Utilizing carbon nanotubes (CNTs) as substitutes for the conventional rigid indium-tin oxide (ITO) electrodes, all CNT based flexible field emission devices (FEDs) were possible to prepare with a novel film transfer method. In the method, both CNT-based flexible cathode and anode were fabricated by first attaching the vacuum filtered CNT film/mixed cellulose eater (MCE) filter membrane to an adhesive semi-cured poly(dimethyl siloxane) substrate, and then peeling off the MCE filter membrane. Effects of bending direction and bending radius on field emission properties were studied. The field emission performance of convex bending device was worse than that of flat device and deteriorated further with the decrease of bending radius. In contrast, the concave bending device exhibited better field emission properties than flat device; nevertheless, its field emission properties decreased as the concave bending radius reduced below a certain value. The method achieved two successes. One is that the interfacial interaction between CNT films and flexible substrate was greatly enhanced. The other is that the transfer process improved the field emission properties due to the increase of vertically aligned CNT tips. Compared with traditional methods applied in FED preparation, the novel modified transfer method is organic free, easy to control, cheap, and environment friendly.

1. Introduction

In recent years, flexible field emission devices (FEDs) have received much attention due to many potential advantages, such as very thin profiles, lightweight, robust display, and especially the ability to flex, curve, conform, roll, and fold [1-7]. Generally, a flexible FED should keep its functionality under various mechanically flexible operations. Therefore, all materials applied to flexible FED should be flexible and the interfacial interactions between materials must be strong. The main components of flexible FED contain an electron emitter layer, the conducting layer and flexible substrate. The emitter is always employed by high aspect ratio nanomaterials such as carbon nanotube (CNT) [3-5, 8-10], ZnO nanowire (NW) [1], Si nanotip [11, 12], SiC NW [2, 13], Au NW [14], Co_5Ge_7 NW [15] and so on. The conducting layer is usually made by graphene [3, 6, 16, 17], flexible carbon cloth [9] and CNT [8]. The electron emitter layer and conducting layer are commonly prepared separately with different materials. For instance, Hwang et al. reported a transparent and flexible field emission cathode with the emitter layer of vertical ZnO NW and the conducting layer of graphene [18]. Arif et al. fabricated the flexible FEDs with the emitter layer of Au NW and the conducting layer of graphene and Ni films [14]. Contrasted to those complicated layers in flexible FED structure, CNT films are suitable for emitter layer as well as conducting layer because of their unique properties of high aspect ratio, low work function, high mechanical strength and high electrical conductivity [19-22]. To simplify the manufacturing process and increase field emission stability, CNT films are promising candidates for emitter layer as well as conducting layer applied in flexible FED to fabricate the all-CNT based flexible FED. Herein, "all-CNT" means that the emitters and the conducting layers of the anode and cathode are all made of CNT films.

On the other hand, deficiency in manufacturing processes hindered the commercialization of flexible FEDs. Because most

substrates of flexible FEDs, such as polyethylene terephthalate (PET), polycarbonate, poly(dimethyl siloxane) (PDMS), and polyethylene naphthalate, are not resistant to high temperature, and the current fabrication processes for rigid FEDs including physical vapor deposition (PVD) [23], chemical vapor deposition (CVD) [24, 25], and screen-printing [21, 26], which mainly relied on high temperature are unsuitable for flexible FEDs. Besides, various low temperature approaches related to rigid FED manufacturing have more or less drawbacks when applied to flexible FEDs. The typical low temperature processes such as electrophoresis [27], spraying [28-30], and dip-coating [5, 31], can be utilized to build FED components. However, CNT films prepared by electrophoresis and spraying have a drawback of film inhomogeneity. More seriously, the interfaces between coating layers (CNT film, phosphor, etc.) and substrates by all three methods have poor adhesion [29, 30, 32]. This is a serious drawback even for rigid FED, let alone flexible FED.

Several improvements and modifications of these methods have been reported to circumvent the high process temperature and/or poor adhesion. By plasma-enhanced CVD, CNT emitter films were grown at low temperatures suitable for use of flexible substrates [4, 33]. However, in contrast to CNTs in a high temperature process, emission stability and current intensity declined due to more defects and amorphous carbon in the CNTs grown at a low temperature [34, 35]. To overcome the weak adhesion of CNTs/polymer in flexible devices, a microwave-welding technique was applied to weld CNT films prepared by spraying or screen-printing onto flexible polymer substrates [36]. However, the length and the density of the welded nanotubes are difficult to control, which might result in poor emission stability.

The above-mentioned approaches can be categorized as one-step technology in which CNT films as emitters or conductive electrodes are grown or formed directly on flexible substrates. It can be seen that one-step technology cannot meet all requirements of flexible FED fabrication. Another general fabrication strategy of CNT emitters and conductive electrodes is a two-step technology. In the two-step technology, CNT films are firstly prepared on temporary substrates under some conditions that are inappropriate for use of flexible substrates but prerequisite for CNT film formation or optimal CNT performance in specific applications. Then as-prepared CNT films are transferred onto the destination substrate under the conditions that are applicable for flexible substrates [37, 38]. For the first step, CVD and vacuum filtering are two typical approaches [37], while the second step can be classified into a solution-based method and a dry transfer printing [37]. In these approaches, vacuum filtering method possesses advantages of high surface homogeneity, easy control of film thickness, low cost, and simplicity. The dry transfer printing method is advantageous over solution-based processing as the etching solution used in wet method may cause more or less damage to CNT films. The two-step technology based on combination of vacuum filtration with dry transferring technique (hereafter referred as vacuum-filtration/dry-transferring) is thus a promising candidate for flexible FED manufacturing. However, flexible FEDs fabricated by vacuum-filtration/dry-transferring have never been reported before.

In the paper, we fabricated all-CNT based flexible FEDs by the two-step vacuum-filtration/dry-transferring method. The dry-transferring method here is based on adhesive viscosity of semi-cured PDMS substrate, instead of the traditional dry transfer printing which is always assistant with a third-party stamp or adhesive layer [37]. This method achieved strong adhesion between CNT films and flexible substrate and was beneficial to form a large number of CNT tips in the cathode, which thus increased the density of electron emitters. Furthermore, the field emission properties of flexible devices with different bending directions and bending radii were systematically investigated.

2. Experimental

2.1 Preparation of all-CNT based flexible anode and cathode

The fabrication processes of all-CNT based flexible FEDs are illustrated in Fig. 1. Both flexible PDMS-based substrates for FED cathode and anode were prepared by semi-curing the mixture of PDMS precursor and a curing agent (10:1) at 60 ^{o}C for 1 h. The semi-cured PDMS based substrate has the properties of high transparency, strong adhesion strength and excellent flexibility. The fabrication processes of all-CNT based flexible FEDs are based on these unique properties. Firstly, single walled CNT (SWCNT) (purchased from Shenzhen Nanotech Port Co., Ltd., purity: CNTs > 95%, diameter < 2 nm, length of 5 – 15 μm) and double walled CNT (DWCNT) (purity: CNTs > 90%, diameter < 5 nm, length of 5 – 15 μm) (see supplementary materials for details analysis by TEM, FTIR and thermal gravity analysis) were dispersed by bath sonication for 1 h in a 1 wt% sodium dodecylbenzene sulfonate solution in separate beakers, respectively. Then after centrifugation at 1000 rpm for 5 min for each solution, the well-dispersed SWCNT solution (0.05 mg/ml) and DWCNT solution (0.2 mg/ml) were obtained. Thereafter the SWCNT and DWCNT solutions were vacuum-filtrated through a mixed cellulose ester (MCE) membrane (pore size of 0.8 μm) to form a SWCNT/MCE structure and a DWCNT/MCE structure, respectively. Subsequently, each of the two structures was stacked with one semi-cured PDMS substrate to form the PDMS/SWCNT/MCE structure and the PDMS/DWCNT/MCE structure. Then a press process was performed individually on each structure to achieve good contact with PDMS substrate. Finally, PDMS/SWCNT structure and PDMS/DWCNT structure were acquired by peeling off each MCE membrane from the PDMS/SWCNT/MCE structure and PDMS/DWCNT/MCE structure, respectively. PDMS/DWCNT structure was used as the flexible cathode, and PDMS/SWCNT structure, after dip-coated with green phosphor and dried at 80 ^{o}C for 4 h, served as flexible transparent conductive anode. Note that the reason why we used the SWCNT film as the transparent anode and the DWCNT film as the field emission cathode is that we found the SWCNT film possesses higher transmittance at similar resistance but weaker field emission performance compared with the DWCNT film. Finally, by printing low temperature silver paste onto the edge of CNT films, the anode and cathode were wired for field emission test.

Cite this: DOI: 10.1039/c0xx00000x

www.rsc.org/xxxxxx

ARTICLE TYPE

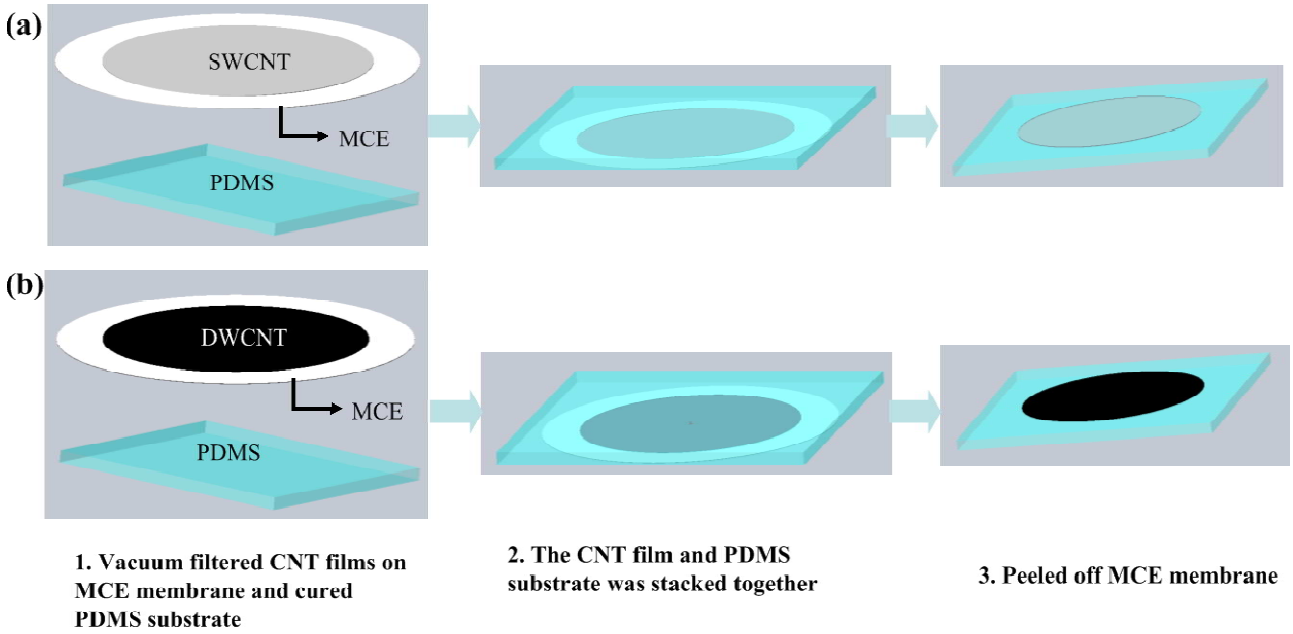

Fig. 1 Schematic of the process flow for fabricating (a) flexible SWCNT-PDMS films for field emission anode and (b) flexible DWCNT-PDMS films for field emission cathode. Herein, the grey color for SWCNT film and the black color for DWCNT film are used only for indicating different transparency.

2.2 Characterization of samples

The morphology of all-CNT based flexible electrodes was examined by field emission scanning electron microscopy (FESEM) using HITACHI S-4800 at a working voltage of 5 kV. Sheet resistance of the film was measured by a four-point probe method with a surface resistivity measurement system (RTS-8). The UV–vis absorption spectra were recorded using a Hitachi U-3900 UV–vis spectrophotometer. Field emission properties were performed in vacuum (6.0×10^{-4} Pa) by a homemade conventional diode-type structure. A 500 μm thick PET spacer was used to keep the distance between cathode and anode.

3. Results and discussion

Figure 2(a) and (b) are FESEM images of DWCNT films on flexible PDMS substrate and MCE membrane, *i.e.* CNT films after and before peeling off MCE, respectively. It can be observed that CNTs are uniformly distributed over the entire area. The CNTs in the films form a network and keep good contact with each other, which implies the excellent electrical conductivity of CNT films. The uniform morphology of CNT films suggests the good electron emission uniformity. The insets of Fig. 2(a) and (b) are the side views of these two samples. From the insets, numerous vertically aligned CNTs are observed on the CNT based flexible cathode, whereas few CNT tips are visible on the CNT films over MCE membrane. The vertically aligned CNT tips served as the main electron emitters in the field emission and the number of them is one of the most important factors influencing the field emission performance. The increase in number of CNT tips hints an improvement of field emission property of DWCNT/PDMS flexible FED. The difference in numbers of the vertically aligned CNT tips between the insets of Fig. 2(a) and (b) is caused by peeling off MCE membrane from the PDMS/CNT/MCE structure. As the activation tape method did [39], the process of peeling off MCE membrane from the PDMS/CNT/MCE structure forms an equivalent density of vertically aligned CNTs. The formation mechanism of these aligned CNTs could be described below. On the interface of CNT film and MCE membrane, a few CNTs seep into the micropores of MCE membrane. It brings a strong adhesion between CNT film and MCE membrane. When the MCE membrane is peeled off from the MCE/CNT/PDMS structure, the CNTs seeped into MCE membrane are also pulled up due to the strong adhesion. Consequently, the pull force between MCE/CNT and CNT/PDMS generates vertically aligned CNT tips on the surface of flexible cathode.

Cite this: DOI: 10.1039/c0xx00000x

www.rsc.org/xxxxxx

ARTICLE TYPE

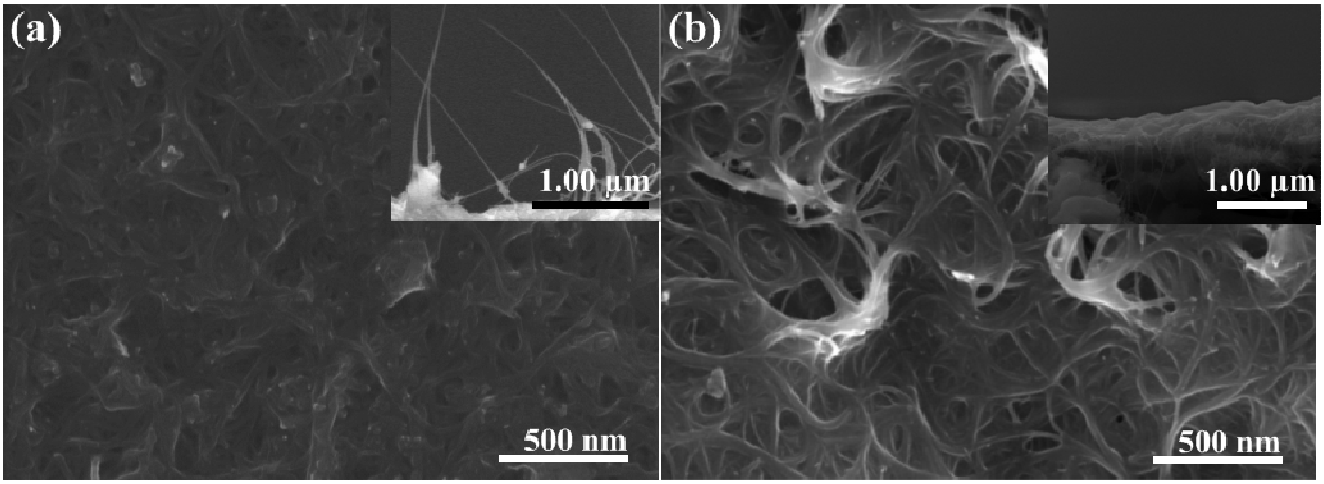

Fig. 2 FESEM images of (a) DWCNT films on flexible PDMS substrate and (b) DWCNT films on MCE membrane. Insets show the side views of DWCNT films on PDMS substrate and MCE membrane.

The morphology of SWCNT based flexible anode is shown in Fig. 3(a). CNT network structure reflects the excellent electron conducting property between CNTs. The SWCNT-based flexible film owns a low sheet resistance of 1.4 kΩ·sq^{-1} and an optical transparency of 58% at 550 nm (Fig. 3(b)), which is in good agreement with inset of Fig. 3(b). These results show that the transfer method is effective in preparing CNT based flexible anode.

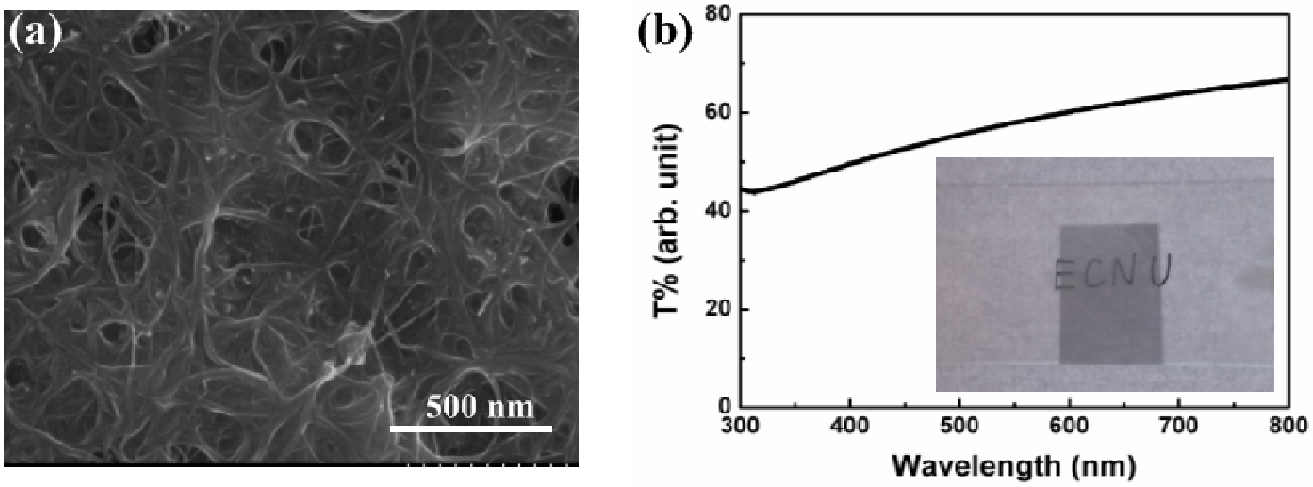

Fig. 3 (a) FESEM image of SWCNT based flexible anode. (b) Transmission spectrum for SWCNT based flexible anode. The inset of (b) demonstrates the optically transparent picture of the flexible anode.

Electron field emission studies of all-CNT based flexible devices with different bending state were performed. The current density versus applied electric field (*J-E*) characteristics of the samples with different bending radius and bending direction are shown in Fig. 4(a). The turn-on field (with a current density of 1 μA·cm^{-2}) and threshold field (with a current density of 0.5 mA·cm^{-2}) of flat sample are 0.56 and 1.02 V·μm^{-1}, which are much lower than those of [40]. Meanwhile, the *J-E* curves are distinctly influenced by bending states. Comparing with the flat sample, the convex bending samples show worse field emission performances, and as the bending radius reduces, the field emission performances turn worse. On the contrary, the field emission performances of concave bending samples are better than that of the flat sample. However, as the concave bending radius reduces from 5.0 to 2.5 cm, the field emission performance decays. The optimized sample is that with a concave bending radius of 5 cm and owns

the lowest turn-on field and threshold field of 0.44 and 0.92 V·μm^{-1}.

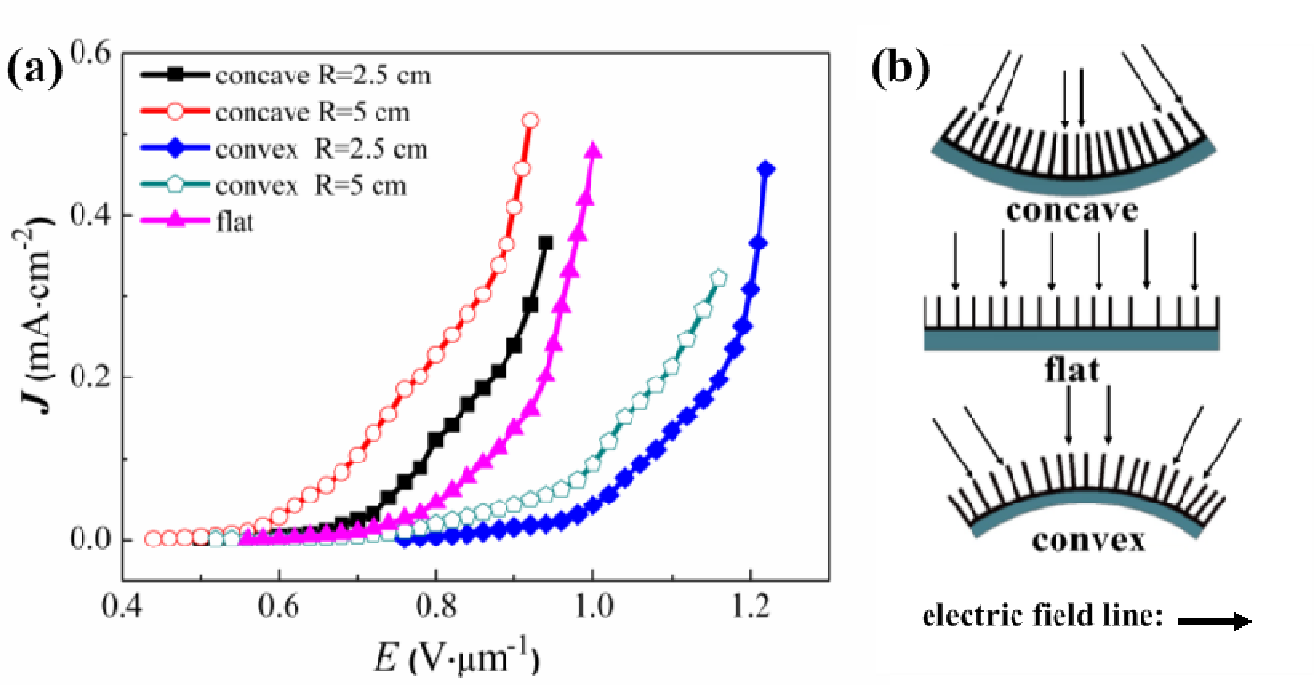

Fig. 4 (a) Emission current density versus applied electric field of all-CNT based flexible FEDs with different bending radii. (b) Schematic of flexible samples with concave, flat, and convex curvatures

The differences of *J-E* performance between flat sample and bending samples are probably caused by two factors: the electron emitter density and the electric field intensity.

One factor, *i.e.* the change of electron emitter density with different bending states, could explain the difference in field emission among the samples with different curvatures. It is well known that nanotube films with low emitter density yield low emission current. In contrast with flat CNT cathode, the density of CNT emitters reduces by convex bending, but increases by concave bending, as shown in Fig. 4(b). Correspondingly, field emission performances of the convex bending samples would get worse, while those of the concave-bending samples become better. However, when the density of CNT emitters is too large, it causes the field screening effect, which suppresses electric field around CNT tips and results in worse FE performance [41, 42]. In our case, the sample with concave bending radius of 2.5 cm, in spite of the highest CNT emitter density, only exhibits medium field emission properties. The field emission properties enhanced not so much as expected, can be attributed to the field screening effect due to high CNT density.

The other factor is that the deformations of flexible anode and flexible cathode change the electric field line density, which denotes the electric field intensity between anode and cathode, as illustrated in Fig. 4(b). Comparing with the flat sample, the electric field lines of the concave bending sample are focused together, which means that the electric field intensity near the cathode is enhanced. In contrast, the electric field intensity of convex bending sample decreases. With the same applied voltage and the same separating spacer between cathode and anode, the electric field intensity increases in the order of convex, flat, and then concave curvatures, making the tendency of turn on field and threshold field opposite.

In order to understand the effect of mechanical deformation of flexible FEDs on field emission, the Fowler–Nordheim (*F-N*) model is introduced to analyze the data in Fig. 4(a). From the *F–N* theory, the field enhancement factor β can be calculated using the equation as follows:

$$J = A\frac{\beta^2 E^2}{\Phi}\exp(-\frac{B\Phi^{1.5}}{\beta E}), \qquad (1)$$

The reduced *F-N* equation developed by Forbes [40] indicates the linear relationship between ln (J/E^2) and $1/E$ as below:

$$\ln(\frac{J}{E^2}) = -6.83\times10^3\frac{\Phi^{1.5}}{\beta E} + C\ , \qquad (2)$$

where J is the emission current density, A = 1.56×10^{-6} A·V^{-2}·eV, B = 6.83×10^9 eV$^{-3/2}$·V·m^{-1} [43], β is the field enhancement factor, Φ is the work function, E is the applied electric field, and C is a constant. Assuming the work function of the CNTs to be 5.0 eV, we plot ln (J/E^2) versus $1/E$ in Fig. 5. The β can be calculated easily by the equation as below:

$$\beta = -6.83\times10^{3}\frac{\Phi^{1.5}}{K}, \qquad (3)$$

where K is the slope of the plot. The sample with a concave bending radius of 5 cm achieves the highest β of 18100, and the value of the flat sample is 11300.

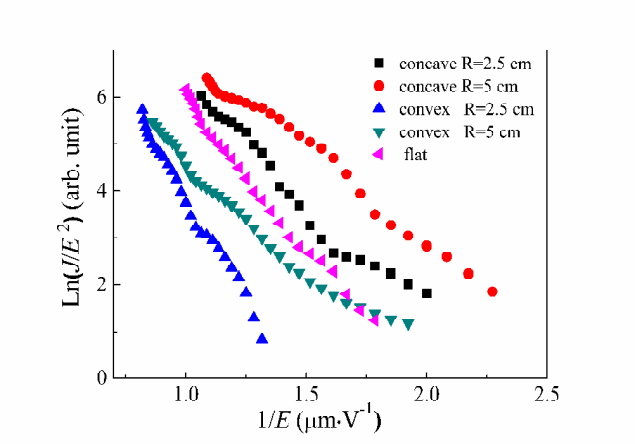

Fig. 5 Fowler-Nordheim (*F-N*) curves of CNT based flexible FEDs with different bending radii.

As one of the best way to estimate the field emission properties, the luminance test can show the samples' field emission uniformity. At a given electric field, the uniformity of CNT emitters can be reflected by luminance uniformity, and the CNT emitter density can be shown by the brightness. We investigated the luminance uniformity and brightness of all-CNT based flexible devices. Figure 6 shows the luminescent pictures of all-CNT based flexible samples with different bending directions and at different applied electric fields. All three samples with good luminance uniformities at 0.95 V·μm^{-1} reveal the excellent uniformity of CNT emission tips under different bending states. Furthermore, the brightness of three samples is greatly increased as the electric field increases from 0.95 to 1.25 V·μm^{-1}, which reflects a high density of electron emitters in high field.

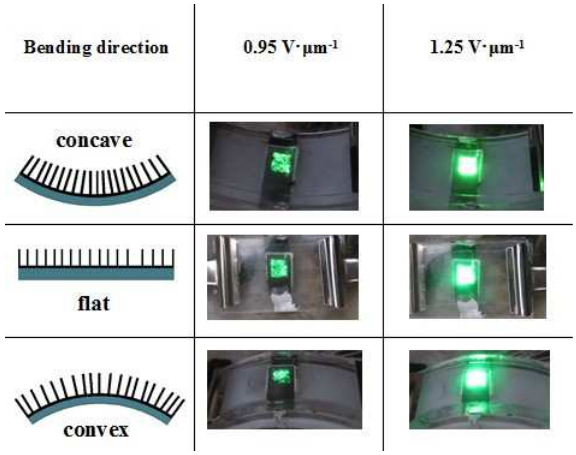

Fig. 6 Luminance pictures of flexible FEDs with bending radius of 5 cm bent in different direction and at different applied electric field

The current stability is another important parameter for FEDs. A good current stability requires that the field emission current density holds stable in a long term at a given electric field. If the current density declines sustainably and obviously in a short time, the devices own poor stability and cannot be industrialized and commercialized. In this experiment, the emission current stability of the flexible devices is evaluated under different bending statuses, as shown in Fig. 7. The initial emission current densities of three samples are all about 0.35 mA·cm^{-2} at different applied electric field. The applied electric field of each sample is kept constant for 360 min. Overall, the current densities of all samples decline quickly at the first 60 min and keep stable for 300 min without further distinct decrease. Generally speaking, the quickly decline of emission current density at the first hour is caused by the degradation of some prominent CNT tips. The stable emission current density after the degradation indicates an excellent stability of field emission performance of flexible FED under different bending states.

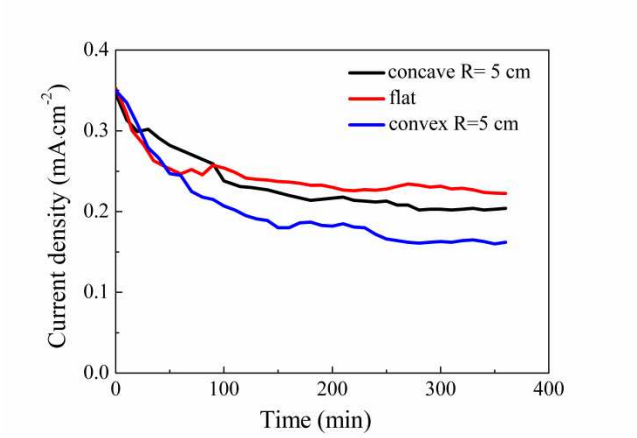

Fig. 7 Emission current stability of all-CNT based flexible FEDs test under different bending states.

Conclusions

Using the promising CNT films as flexible (transparent) electrodes instead of traditional ITO, and combining vacuum filtration with dry transferring techniques for the fabrication of flexible SWCNT anode electrode and DWCNT cathode emitters, we prepared all-CNT flexible FEDs. The devices by this two-step technology showed high flexibility in field emission characteristics with high current density, low turn-on field, high luminance uniformity, and long-term emission stability. The device with a concave bending radius of 5 cm exhibited the best electron emission performance with a low turn-on field of 0.44 V·μm^{-1} and a high field enhancement factor β of 18100. All-CNT flexible FEDs prepared in this report, due to the advantages of environment friendliness, low-cost, and strong adhesion strength between CNT films and substrates, as well as good field emission properties, excellent uniformity, and long-term emission stability, indicated a possibility of their commercial application.

Acknowledgments

This work was partly supported by Shanghai Nanotechnology Promotion Center (12nm0503801), National Natural Science Foundation of China (11204082 and 51102095), the Natural Science Foundation of Zhejiang Province, China (Z1110057) and Research Fund for the Doctoral Program of Higher Education of China (20110076120023).

Notes

[a] *Engineering Research Center for Nanophotonics & Advanced Instrument, Ministry of Education, Department of Physics, East China Normal University, 3663 North Zhongshan Road, Shanghai 200062, China*

**Pingsheng Guo*
Fax: +86-21-62234321; Tel: +86-21-62232054; E-mail: psguo@phy.ecnu.edu.cn
** Wei Ou-Yang*
Fax: +86-21-62234321; Tel: +86-21- 62233673; E-mail: ouyangwei@phy.ecnu.edu.cn

[b] *Herbert Gleiter Institute of Nanoscience, Nanjing University of Science & Technology, 200 Xiaolinwei Road, Nanjing 210094, China*

[c] *Department of Physics, Zhejiang University, 38 ZheDa Road, Hangzhou 310027, China*

References

1 C.-L. Hsu, C.-W. Su and T.-J. Hsueh, *RSC Advances*, 2014, **4**, 2980.

2 S. Chen, P. Ying, L. Wang, F. Gao, G. Wei, J. Zheng, Z. Xie and W. Yang, *RSC Advances*, 2014, **4**, 8376.

3 D. H. Lee, J. A. Lee, W. J. Lee and S. O. Kim, *Small*, 2011, **7**, 95.

4 S. Hofmann, C. Ducati, B. Kleinsorge and J. Robertson, *Applied Physics Letters*, 2003, **83**, 4661.

5 O.-J. Lee and K.-H. Lee, *Applied Physics Letters*, 2003, **82**, 3770.

6 V. P. Verma, S. Das, I. Lahiri and W. Choi, *Applied Physics Letters*, 2010, **96**, 203108.

7 T. T. Tan, H. S. Sim, S. P. Lau, H. Y. Yang, M. Tanemura and J. Tanaka, *Applied Physics Letters*, 2006, **88**, 103105.

8 H. J. Jeong, H. D. Jeong, H. Y. Kim, J. S. Kim, S. Y. Jeong, J. T. Han, D. S. Bang and G.-W. Lee, *Advanced Functional Materials*, 2011, **21**, 1526.

9 N. Liu, G. Fang, W. Zeng, H. Zhou, H. Long and X. Zhao, *Journal of Materials Chemistry*, 2012, **22**, 3478.

10 A. Jha, U. K. Ghorai, D. Banerjee, S. Mukherjee and K. K. Chattopadhyay, *RSC Advances*, 2013, **3**, 1227.

11 W.-C. Yen, H. Medina, C.-W. Hsu and Y.-L. Chueh, *RSC Advances*, 2014, **4**, 27106.

12 T. Chang, F. Lu, S. Kunuku, K. Leou, N. Tai and I. Lin, *RSC Advances*, 2014, **5**, 2928.

13 S. Chen, P. Ying, L. Wang, G. Wei, J. Zheng, F. Gao, S. Su and W. Yang, *Journal of Materials Chemistry C*, 2013, **1**, 4779.

14 M. Arif, K. Heo, B. Y. Lee, J. Lee, D. H. Seo, S. Seo, J. Jian and S. Hong, *Nanotechnology*, 2011, **22**, 355709.

15 H. Yoon, K. Seo, N. Bagkar, J. In, J. Park, J. Kim and B. Kim, *Advanced Materials*, 2009, **21**, 4979.

16 D. D. Nguyen, Y.-T. Lai and N.-H. Tai, *Diamond and Related Materials*, 2014, **47**, 1.

17 I. Lahiri, V. P. Verma and W. Choi, *Carbon*, 2011, **49**, 1614.

18 J. O. Hwang, D. H. Lee, J. Y. Kim, T. H. Han, B. H. Kim, M. Park, K. No and S. O. Kim, *Journal of Materials Chemistry*, 2011, **21**, 3432.

19 W. I. Milne, K. B. K. Teo, M. Chhowalla, G. A. J. Amaratunga, S. B. Lee, D. G. Hasko, H. Ahmed, O. Groening, P. Legagneux, L. Gangloff, J. P. Schnell, G. Pirio, D. Pribat, M. Castignolles, A. Loiseau, V. Semet and V. Thien Binh, *Diamond and Related Materials*, 2003, **12**, 422.

20 D. H. Shin, S. I. Jung, K. N. Yun, G. Chen, Y.-H. Song, Y. Saito, W. I. Milne and C. J. Lee, *Applied Physics Letters*, 2014, **105**, 033110.

21 J. Xu, R. Pan, Y. Chen, X. Piao, M. Qian, T. Feng and Z. Sun, *Journal of Alloys and Compounds*, 2013, **551**, 348.

22 G. Sanborn, S. Turano and W. J. Ready, *Diamond and Related Materials*, 2014, **43**, 1.

23 K. A. Sierros, D. S. Hecht, D. A. Banerjee, N. J. Morris, L. Hu, G. C. Irvin, R. S. Lee and D. R. Cairns, *Thin Solid Films*, 2010, **518**, 6977.

24 X. Xu and G. R. Brandes, *Applied Physics Letters*, 1999, **74**, 2549.

25 A. V. Melechko, V. I. Merkulov, T. E. McKnight, M. A. Guillorn, K. L. Klein, D. H. Lowndes and M. L. Simpson, *Journal of Applied Physics*, 2005, **97**, 041301.

26 P. S. Guo, T. Chen, Y. W. Chen, Z. J. Zhang, T. Feng, L. L. Wang, L. F. Lin, Z. Sun and Z. H. Zheng, *Solid-State Electronics*, 2008, **52**, 877.

27 W. B. Choi, Y. W. Jin, H. Y. Kim, S. J. Lee, M. J. Yun, J. H. Kang, Y. S. Choi, N. S. Park, N. S. Lee and J. M. Kim, *Applied Physics Letters*, 2001, **78**, 1547.

28 R. C. Tenent, T. M. Barnes, J. D. Bergeson, A. J. Ferguson, B. To, L. M. Gedvilas, M. J. Heben and J. L. Blackburn, *Advanced Materials*, 2009, **21**, 3210.

29 H. J. Jeong, H. K. Choi, G. Y. Kim, Y. I. Song, Y. Tong, S. C. Lim and Y. H. Lee, *Carbon*, 2006, **44**, 2689.

30 Y. D. Lee, K.-S. Lee, Y.-H. Lee and B.-K. Ju, *Applied Surface Science*, 2007, **254**, 513.

31 S. J. Oh, Y. Cheng, J. Zhang, H. Shimoda and O. Zhou, *Applied Physics Letters*, 2003, **82**, 2521.

32 S. C. Lim, H. K. Choi, H. J. Jeong, Y. I. Song, G. Y. Kim, K. T. Jung and Y. H. Lee, *Carbon*, 2006, **44**, 2809.

33 S. Hofmann, C. Ducati, J. Robertson and B. Kleinsorge, *Applied Physics Letters*, 2003, **83**, 135.

34 S.-J. Kyung, Y.-H. Lee, C.-w. Kim, J.-H. Lee and G.-Y. Yeom, *Carbon*, 2006, **44**, 1530.

35 C. Jin, J. Wang, M. Wang, J. Su and L.-M. Peng, *Carbon*, 2005, **43**, 1026.

36 C. Y. Wang, T. H. Chen, S. C. Chang, T. S. Chin and S. Y. Cheng, *Applied Physics Letters*, 2007, **90**, 103111.

37 Y. Zhou, L. Hu and G. Grüner, *Applied Physics Letters*, 2006, **88**, 123109.

38 Y. Sun and H. H. Wang, *Advanced Materials*, 2007, **19**, 2818.

39 T. J. Vink, M. Gillies, J. C. Kriege and H. W. J. J. van de Laar, *Applied Physics Letters*, 2003, **83**, 3552.

40 T. Y. Tsai, C. Y. Lee, N. H. Tai and W. H. Tuan, *Applied Physics Letters*, 2009, **95**, 013107.

41 X. D. Wang, J. Zhou, C. S. Lao, J. H. Song, N. S. Xu and Z. L. Wang, *Advanced Materials*, 2007, **19**, 1627.

42 H. Zeng, X. Xu, Y. Bando, U. K. Gautam, T. Zhai, X. Fang, B. Liu and D. Golberg, *Advanced Functional Materials*, 2009, **19**, 3165.

43 C. X. Xu and X. W. Sun, *Applied Physics Letters*, 2003, **83**, 3806.